Visual pigments, ocular filters and the evolution of snake vision

Bruno F. Simões[1,*], Filipa L. Sampaio[1], Ronald H. Douglas[2], Ullasa Kodandaramaiah[3], Nicholas R. Casewell[4], Robert A. Harrison[4], Nathan S. Hart[5], Julian C. Partridge[6], David M. Hunt[6,7] & David J. Gower[1,*].

[1]Department of Life Sciences, The Natural History Museum, London, SW7 5BD, UK; [2]Department of Optometry and Visual Science, City University London, London EC1V 0HB, UK; [3]School of Biology, Indian Institute of Science Education and Research Thiruvananthapuram, Thiruvananthapuram 695 016, India; [4]Alistair Reid Venom Research Unit, Liverpool School of Tropical Medicine, Pembroke Place, Liverpool L3 5QA, UK; [5]Department of Biological Sciences, Macquarie University, North Ryde, NSW 2109, Australia; [6]School of Animal Biology and The Oceans Institute, The University of Western Australia, Perth, WA 6009, Australia; [7]Lions Eye Institute, University of Western Australia, Perth, 6009, Australia

*Email: bruno.simoes@me.com; d.gower@nhm.ac.uk

Abstract

Much of what is known about the molecular evolution of vertebrate vision comes from studies of mammals, birds and fish. Reptiles (especially snakes) have barely been sampled in previous studies despite their exceptional diversity of retinal photoreceptor complements. Here we analyse opsin gene sequences and ocular media transmission for up to 69 species to investigate snake visual evolution. Most snakes express three visual opsin genes (*rh1, sws1, lws*). These opsin genes (especially *rh1* and *sws1*) have undergone much evolutionary change, including modifications of amino acid residues at sites of known importance for spectral tuning, with several tuning site combinations unknown elsewhere among vertebrates. These changes are particularly common among dipsadine and colubrine 'higher' snakes. All three opsin genes are under purifying selection, though dN/dS varies with respect to some lineages, ecologies, and retinal anatomy. Positive selection was detected at multiple sites in all three opsins, these being concentrated in transmembrane domains and thus likely to have a substantial effect on spectral tuning and other aspects of opsin function. Snake lenses vary substantially in their spectral transmission. Snakes active at night and some of those active by day have very transmissive lenses, while some primarily diurnal species cut out shorter wavelengths (including UVA). In terms of retinal anatomy, lens transmission,

visual pigment spectral tuning and opsin gene evolution the visual system of snakes is more diverse than in any other tetrapod order.

Key words: ocular media, sensory evolution, photoreception, Serpentes, spectral tuning, vision

Introduction

Animal vision has become one of the best examples of the power of integrative biology. A great deal is known about the anatomy of eyes at many levels, but much is also known about how eyes function and have evolved, including aspects of the physiology underlying photon capture, spectral sensitivity, signal transduction and propagation, and the identity of several key genes and proteins. Indeed, vision is one of the best characterized of all biological sensory systems. In addition, selective pressures can often be determined from physical first principles, allowing the identification and quantification of many aspects of the evolution of eyes (Land 1981; Nilsson 1996). In general, vision in vertebrates is especially well studied, and studies of the evolution of their visual pigments have been able to both identify evolutionary changes, and to ascribe such changes to adaptive evolutionary processes (e.g. Hughes 2008).

The fundamentals of vertebrate vision have been particularly well studied in terms of the molecular basis of photoreception and phototransduction. A cornerstone of this is knowledge of the photosensitivity of visual pigments, members of the large family of G-protein-coupled-receptor (GPCR) proteins, which share a common arrangement of an opsin protein linked to a chromophore derived from vitamin A (Wald 1968). Visual pigments play a core role in photon detection and colour vision and they are a leading example of how gene duplications (Dulai et al. 1999) and changes in amino acid sequences (Yokoyama 2008), type of chromophore (vitamin A1 or A2: Enright et al. 2015) and gene expression (Hofmann and Carleton 2009; Carleton et al. 2010) underlie adaptations to differing ecological and behavioural selection pressures. Visual opsins in some vertebrates have been intensely studied over the past 20 years, to the extent that changes in specific amino acid ('spectral tuning') sites are known to change the peak absorbance wavelength (λ_{max}) of the visual pigments (Yokoyama 2008; Yokoyama et al. 2014). However, there is no universal consensus about the tuning impacts of all such mutations (Hauser et al. 2014), with some data suggesting that additional mechanisms to change spectral sensitivity may exist (Davies et al. 2009; Martin et al. 2015).

Much of our knowledge about the function and evolution of vertebrate vision, including its molecular basis, comes from empirical studies on a relatively small proportion of living vertebrates, predominantly some groups of mammals, birds and fish (Nickle and Robinson 2007; Davies et al. 2012). Investigation of vision in other

vertebrates is needed to test inferred generalities, especially in those taxa having visual systems with very different anatomical arrangements of the eye, and/or great phenotypic diversity. Snakes are one such lineage that shows substantial diversity of ocular anatomy, especially retinal photoreceptor complement. Indeed, Walls (1942) and Underwood (1967; 1970) argued that, by virtue of their great diversity of photoreceptor complements, there must have been more evolutionary changes within snakes than in all the other vertebrates combined. The eyes of snakes are also remarkable for being highly divergent in gross morphology from that of non-snake squamates ('lizards'), in lacking photoreceptor oil droplets, in mostly being covered by a transparent head scale (spectacle or Brille), and in presenting evidence for evolutionary transitions ('transmutation' sensu Walls 1934) between rods and cones (Walls 1942).

The approximately 3,500 species of living snakes are distributed across all continents except Antarctica (Van Wallach et al. 2014). They are very diverse ecologically (e.g., Greene 1997) and include burrowing, arboreal, gliding, fully aquatic, nocturnal and diurnal species. Some have small eyes lying under typical head scales, while others are visual hunters with well developed binocular vision, some of which have horizontal pupils and a fovea (Walls 1942). Since Walls' and Underwood's pioneering anatomical surveys, we have learned that the ancestral snake likely had three of the five visual opsin genes present in the ancestral vertebrate (Davies et al. 2009; Simões et al. 2015), but not much more is known.

In order for light to be absorbed by the visual pigments it first has to pass through the ocular media. In vertebrates these comprise the cornea, lens, and aqueous and vitreous humour. Snakes additionally have a covering over the cornea (brille or spectacle). Lens transmission characteristics of most major vertebrate groups have been widely studied (e.g. Douglas and Marshall 1999; Douglas and Jeffery 2014 for reviews), but there are few reports of the spectral transmission of snake lenses. Walls (1931) noted yellow (blue-absorbing) lenses in a number of diurnal snakes and uncoloured lenses in nocturnal species. However, these observations were qualitative, using the UV-insensitive human visual system, such that the spectral characteristics of both coloured and transparent lenses in the UV are unknown, with the exception of two species of sea snake whose lenses transmit significant amounts of UV (Hart et al. 2012). The spectral characteristics of the reptilian spectacle have been reported only twice (Hart et al. 2012; van Doorn and Sivak 2015).

Given the anatomical diversity of snake retinal photoreceptors and the relative lack of previous studies, we address the following major questions: (1) What are the major patterns in the diversity and molecular evolution of snake visual opsins? (2) Is the diversity in retinal photoreceptor anatomy, visual opsin and ocular media transmission

linked in a predictable way? (3) To what extent is visual opsin spectral tuning and/or opsin molecular evolution explained by major shifts in ecology and/or retinal anatomy? (4) Do snakes present diversity in visual opsins beyond that known for other major groups of vertebrates, mirroring the diversity of their ocular morphology?

Here we report the largest dataset of visual opsin genes in reptiles to date, covering the major types of snake retinal anatomy and taxonomic and ecological diversity. We also report data on the spectral transmission of important components of the ocular media (lens and spectacle) of a subset of these snakes. We find that although the vast majority of snakes retain three of the visual opsin genes likely present in the ancestral snake, these have undergone considerable diversification through functionally important amino acid substitutions. Notably, many of these substitutions are unreported in other vertebrate groups. There are also changes in the transmission of the lens, particularly with respect to the filtering of short wavelengths that will significantly affect overall spectral sensitivities. Snakes are an important system for understanding of the evolution of the vertebrate visual system.

Material & Methods

Taxon sampling and sample storage

Snakes were acquired through fieldwork, the Liverpool school of Tropical Medicine, from hobbyists and the commercial trade. Our sampling (SI Table S1) aimed to maximise taxonomic (phylogenetic), ecological and ocular anatomical diversity. One specimen each of 48 species was newly sampled. The use of animals in this research was conducted using standard protocols approved by the Liverpool school of Tropical Medicine Animal Welfare and Ethical Review Board and the UK Home Office. Following euthanasia, spectacle scales (brilles) were removed and the eyes extracted. After removing the lens, each eye was coarsely macerated and stored in RNAlater (Ambion) at -80°C until the RNA extraction. Where possible, undamaged lenses and spectacles were stored dry at -20°C until measurement of spectral transmission was performed.

RNA extraction and cDNA synthesis

Total RNA was extracted from eyes using TRIzol® (Life Technologies/Ambion) followed by purification with PureLink™ RNA Mini Kit (Life Technologies/Ambion) using the manufacturer's protocol. First-strand complementary DNA (cDNA) was synthesized with a Transcriptor First Strand cDNA Synthesis Kit (Roche) with 500ng of total RNA according to manufacturer's instructions. RNA complementary to the cDNA was removed using 2

146 units of *E. coli* RNase H (Ambion) and incubated at 37°C for 20 minutes. For the
147 following species freshly synthesized cDNA was dehydrated, stored at ambient
148 temperature for 24 hours, and returned to -20°C and rehydrated after a further 24
149 hours before subsequent amplification: *Melanophidium* sp., *Uropeltis* cf. *macrolepis*,
150 *Gongylophis conicus, Pareas monticola, Amphiesma stolata, Xenochrophis piscator,*
151 *Xylophis captaini, Boiga forsteni, Boiga ceylonensis.* All other cDNA samples were kept
152 hydrated and stored at -20°C prior to amplification.

153

154 *Visual opsin gene amplification and cloning*

155 Here we denote opsin genes in lower case italics and opsin proteins in upper case (e.g.
156 *rh1* and RH1, respectively). We amplified the coding regions of *sws1, lws* and *rh1* visual
157 opsin genes using universal primers designed to amplify visual opsin genes across snakes
158 and squamates (Simões et al. 2015). All fragments were amplified in 25 µl Polymerase
159 Chain Reactions (PCR): 1x PCR buffer (Invitrogen), 1.5 mmol (mM) of $MgCl_2$ (Invitrogen),
160 50 µmol/L of deoxynucleotides (Bioline), 0.4 µmol/L of each primer and 1 unit Platinum
161 Taq Polymerase (Invitrogen) and 100ng of cDNA. PCR products were amplified by
162 touchdown PCR with the following cycling parameters: initial denaturation at 95°C for 5
163 minutes; 20 cycles of 1 minute at 95°C (denaturation), 30 seconds at 60°C (annealing),
164 and 1 minute at 72°C (extension) with a decrease of 0.5°C per cycle; 15 cycles of 1
165 minute at 95°C (denaturation), 30 seconds at 50°C (annealing), and 1 minute at 72°C
166 (extension) followed by a final extension at 72°C for 5 minutes. PCR products were run
167 on a 1% agarose gel, excised in a Blue Light Transilluminator (Safe Imager, Invitrogen)
168 and purified with a PureLink Quick Gel Extraction Kit (Invitrogen). PCR fragments were
169 cloned with a StrataClone PCR Cloning Kit (Agilent) and corresponding chemically
170 competent cells following the manufacturer's protocol. Transformed cells were grown
171 overnight on agar medium treated with 100 mg/ml of Ampicilin (Bioline) and 1ml of 2%
172 X-GAL at 37°C. Sixteen white colonies were picked and used as DNA template in 25µl
173 PCR reactions: 1x PCR buffer (Bioline), 1 mmol (mM) of $MgCl_2$ (Bioline), 80 µmol/L of
174 deoxynucleotides (Bioline), 0.2 µmol/L of M13F and M13R vector primers and 1 unit of
175 BioTAQ Polymerase (Bioline) and 2µl of DNA (1 colony twirled in 50µl of ultra-pure
176 water). The PCR had the following cycling parameters: initial denaturation at 95°C for 10
177 minutes; 30 cycles of 15 seconds at 95°C (denaturation), 30 seconds at 58°C (annealing),
178 and 1 minute and 30 seconds at 72°C (extension) and a final extension at 72°C for 1.5
179 minutes. Between four and eight positive clones were sequenced in both directions with
180 M13 universal primers in an automated DNA sequencer. Sequences were assembled in
181 Geneious R8 (Kearse et al. 2012) and are deposited in GenBank, accession numbers
182 XXXX-XXXX (SI Table S1).

Barcoding

Genomic DNA (gDNA) was extracted from each eye tissue sample using the DNA layer in Trizol of the RNA extraction, following the Trizol manufacturer's instructions and/or from muscle tissue stored in ethanol using the Qiagen blood and tissue kit. We generated mitochondrial *16s rRNA* 'barcodes' for most specimens (SI Table S1) using universal primers (Palumbi, 1996) in 25 µl PCR reactions: 1x PCR buffer (Invitrogen), 1 mmol (mM) of $MgCl_2$ (Invitrogen), 50 µmol/L of deoxynucleotides (Bioline), 0.4 µmol/L of each primer and 1 unit Platinum Taq Polymerase (Invitrogen) and 100ng of gDNA. The PCR cycling parameters were: initial denaturation at 95°C for 10 minutes; 30 cycles of 15 seconds at 95°C (denaturation), 30 seconds at 55°C (annealing), and 1 minute at 72°C (extension) and a final extension at 72°C for 1 minute. All successfully amplified products were sequenced in both directions using the same primers used for PCR, in an automated DNA sequencer. The barcodes were assembled in Geneious R8.

Phylogenetic analysis

Visual opsin gene cDNA sequences were aligned with published sequences from other reptiles including other snakes (SI, Table S1) with MAFFT (Katoh et al. 2002) (settings: algorithm; auto; gap penalty: 3; off-set value: 0.1) implemented in Geneious R8, Muscle (Edgar, 2004) (default settings: 15 interactions), and PRANK (Löytynoja & Goldman, 2005) (HKY model with empirical base frequencies and kappa=2). These alignments were inspected by eye for both nucleotides and amino acids and was adjusted manually to ensure nucleotides were in-frame and that indels did not include partial codons. The final alignments based on the results of all three programs were identical. jModelTest 2 (Darriba et al. 2012) was used to ascertain the best-fit model of sequence evolution for each alignment according to their AIC and BIC scores. GTR+G+I was the best-fitting model for the three visual opsin genes amplified. Given concerns about incorrectly estimating G when including I in the model (Yang, 2006), we also ran analyses under GTR+G. Phylogenetic analyses were conducted using Maximum (ML) Likelihood and Bayesian Inference (BI) approaches. ML analyses were run with RAxML v8 (Stamatakis 2014) using majority rule bootstopping criteria (Pattengale et al. 2009); randomized MP starting trees, and a fast hill-climbing algorithm. BI analyses were run with Mr. Bayes v3.1.2 (Huelsenbeck and Ronquist 2001) for 1,000,000 generations with chains sampled every 100 generations (after 25% of trees were discarded as burn-in), random starting trees, 4 chains (3 hot and 1 cold), and convergence was assumed when the standard deviation of split frequencies fell below 0.01. Gekkota was used as the outgroup to root

the *sws1* and *lws* trees, and other non-snake squamate visual opsin gene sequences were used to root the *rh1* tree (SI Table S1).

Analyses of molecular evolution

We used selection test analyses to identify patterns in visual opsin gene evolution across the snake evolutionary tree (using branch models) and within the individual visual opsin genes (site models). Codeml implemented in the PAML 4.7 package (Yang 2007) was used to estimate non-synonymous (dN) and synonymous (dS) substitution rates and the respective ratio (dN/dS, or ω) for the *sws1, lws* and *rh1* genes in snakes. Sequence alignment indels were removed if present in only one taxon or recoded as missing data if present in more.

Branch models (Yang 1998) allow the ω ratio to vary across branches in the tree and can be used to infer positive selection (ω>1) acting in particular lineages. The simplest branch model (one-ratio) allows only one ω ratio value across the tree, whereas the more complex free-ratio model assumes independent ω ratios for each branch. Branch models were also used to estimate ω for two branch categories based on ecotypes (primarily fossorial or not, aquatic/semiaquatic or not, primarily arboreal or not, primarily diurnal or not). The ecological classification applied to each species is reported in Fig. 1 and Table S2. Given the substantial diversity of retinal morphology, ecology and density of our sampling within the family, we also estimated two-ratio branches within Colubridae alone. All branch models were compared using the Likelihood Ratio Test (LRT) and the simpler model (one-ratio) was rejected where $p<0.05$. Branch models were also carried out for a subset of taxa for which the photoreceptor cell complement is known (SI Table S2) to test for possible links between molecular evolution and the presence/absence of double cones or transmuted (sensu Walls 1934) rod-like cones. Retinal anatomy is not known for all species sampled so we removed such taxa from the data set for corresponding molecular evolution analyses and pruned them from the phylogeny in investigations of the relationship between opsin gene evolution and retinal morphology.

Site models (M1a nearly-neutral and M2a positive selection; M7β and M8 β&ω) allow ω to vary among sites (amino-acids or codons) (Yang et al. 2000). Site models M2a and M8 were compared (using LRT) with the simpler site models M1a and M7, respectively and the simpler models rejected where $P>0.05$. Bayes empirical Bayes (BEB) (Yang et al. 2005) implemented in models M2a and M8 β&ω was used to identify sites inferred to be under positive selection for each visual opsin gene.

Under branch-site models, ω can vary across both sites and lineages (Zhang 2005) and this was used to infer positive selection at sites among major lineages of snakes (Colubridae, snakes with transmuted, rod-like cones and snakes that are primarily fossorial, arboreal, aquatic/semiaquatic and diurnal). Branch-site models were compared with the simplest model M1a using LRT. Ancestral visual opsin gene sequences were estimated by marginal and joint reconstruction using Codeml.

We used PRIME analysis executed on the Datamonkey server (Delport et al. 2010) to estimate amino acid exchangeability (as in BEB) but also radical substitutions that result in amino acids with very different biochemical properties. We used both sets of five amino-acid properties available in PRIME: Conant-Stadler (Conant et al. 2007) and Atchley et al. (Atchley et al. 2005). CMS (Delport et al. 2010) was used to identify the most appropriate codon model for PRIME analysis.

For analyses of molecular evolution and ancestral state reconstruction we used a phylogenetic tree congruent with those published by (Wiens et al. 2012; Pyron et al. 2013; Reeder et al. 2015) (Species Tree, Figure 1). Although the monophyly of the colubrid clades Colubrinae, Natricinae and Dipsadinae are well supported (e.g., Wiens et al. 2012; Pyron et al. 2013), there is currently no compelling resolution of the relationships among them. Thus, as well as following the weakly supported resolution in the trees of (Pyron et al. 2013) (Colubrinae lying outside Natricinae+Dipsadinae), we accounted for phylogenetic uncertainty and repeated the branch and site model analyses for the two alternative phylogenetic resolutions: ((Dipsidinae, Colubrinae), Natricinae) and ((Natricinae, Colubrinae), Dipsidinae). The Indian snake *Xylophis captaini* or any congeners have not yet been included in molecular phylogenetic analyses. Although some workers have reported similarities between *Xylophis* and xenodermatids (e.g,. McDowell 1987), we consider the similarity to the Sri Lankan *Aspidura* suggestive of phylogenetic affinity (e.g., Gans 1982; Gower and Winkler 2007) and so we include it as a correspondingly resolved natricine here.

Chi-squared tests of null hypotheses that sites inferred to be under positive selection do not occur unevenly among functional bipartitions (trans-membrane domains; extra- and intracellular loops) of opsins were conducted online at graphpad.com. These tests used one degree of freedom and expected values were calculated under the assumption that sites inferred to be under positive selection are distributed randomly between the functional bipartitions (i.e., in proportion to the total number of sites in each partition). A significance level of $p = 0.05$ was applied.

Estimating visual pigment λ_{max}

It is possible, to some extent, to predict peak absorbance (λ_{max}) of visual pigments from amino acid sequences of their constituent opsins. Such predictions are possible because correlations exist between amino acid sequences of opsins and λ_{max} of corresponding pigments where this has been measured directly in photoreceptors or where opsin genes have been cloned and pigments regenerated *in vitro*. We made predictions of λ_{max} by assuming a vitamin A1 chromophore (A2 chromophores have not been reported in snakes (Davies et al. 2009, Hart et al., 2012, Schott et al. 2015, Sillman et al. 1997, Simões et al. 2015, 2016) and assessing combinations of amino acids at 'spectral tuning' sites known to be especially important in determining λ_{max} in other vertebrates (see Yokoyama 2008 and references cited therein). Predicting λ_{max} based on selected (spectral tuning) amino acid sites is somewhat controversial because additional tuning sites and different tuning mechanisms might remain undiscovered (Hauser et al. 2014). The limited MSP data published thus far for snake visual pigments generally match predictions based on known tuning sites in other vertebrates (e.g. Davies et al. 2009, Simões et al. 2015, 2016). However, we were unable to make confident λ_{max} predictions in cases in which we found spectral tuning amino acids (or combinations thereof) not reported in other vertebrates, or where they occur in other vertebrates but in pigments for which λ_{max} has not been measured.

Ocular media spectral transmission

We examined spectral transmission of lenses and spectacles. Corneas and humours were not scanned because, with the exception of some fish corneas (Kondrasiv et al. 1986; Douglas and McGuigan 1989; Siebeck and Marshall 2000), the vertebrate lens always removes more shortwave radiation than either the cornea or humours (Douglas and Marshall 1999; Douglas and Jeffery 2014). Lenses, and some spectacle samples were thawed and briefly rinsed in phosphate-buffered saline (PBS) and mounted in purpose-built holders in air in front of a Shimadzu ISR 260 integrating sphere within a Shimadzu UV-2101PC spectrophotometer. Transmission at 700 nm was set to 100% and ocular media scanned at 1 nm intervals from 300 to 700 nm. We averaged the measurements of both eyes unless we had only one usable spectacle scale or lens. The lenses were small, 1–3 mm diameter (SI Table S22), limiting the amount of light transmitted through the measuring system, and the use on an integrating sphere reduced sensitivity further, thus the raw data are noisy at short wavelengths where lamp output is low. Data from scans were therefore smoothed using a cubic Savitzky-Golay filter (data frame length 51nm) using Matlab R2011a (The MathWorks Inc, MA, USA). The 50% cut-off wavelength ($\lambda_{50\%}$), the wavelength at which transmission is 50%, was determined for each sample and rounded to the nearest integer. The proportion of UVA (315–400 nm) transmission was calculated for each lens and spectacle following (Douglas and Jeffery 2014). $\lambda_{50\%}$ and %UVA values were plotted for primarily diurnal and

nocturnal species using the package ggplots2 (Wickham 2010) implemented in R (Team 2014) (R Core Team, 2014).

Results

We sequenced approximately 1100bp of cDNA for each of the three visual opsin genes, *sws1*, *lws* and *rh1* found in 48 snake species. Almost the entire coding region for *sws1*, *lws* and *rh1* was amplified and sequenced in the vast majority of species newly sampled. We amplified *rh1* in *Boiga ceylonensis* and *Macroprotodon brevis* (based on single gel bands of approximate expected fragment size) and perhaps *Phyllorhynchus decurtatus* (occasional multiple gel bands in 10 PCRs with various primer and annealing temperature combinations) but sequencing failed. We failed to amplify *rh1* in *Malpolon monspessulanus, sws1* in *Pareas monticola, Boiga ceylonensis* and *B. forsteni,* and *lws* in *Melanophidium* sp. and *Pareas monticola.* In each case between four and fourteen PCRs were repeated using various combinations of primers and annealing temperatures. With one exception (*M. monspessulanus*), the lack of amplification in the latter cases occurred in samples in which the cDNA was temporarily dehydrated, so the failed PCRs may be an artefact. With the addition of the visual opsin gene cDNA sequences previously published for other snakes, the dataset includes 69 snake species covering most major lineages, and representing a broad range of ecologies and retinal anatomies. Spectral transmission was determined for lenses and spectacles of 18 and 15 snake species, respectively.

Functionality and spectral sensitivity

The residues present at amino acid sites of known functional importance for spectral tuning of the visual pigments are reported in SI Tables S3–5. Predictions of visual pigment λ_{max} values are based on the assumed presence of a vitamin A1-derived chromophore; an A2 chromophore is not known in snakes but has been reported for some lizards (e.g. Martin et al. 2015). For *rh1* sequences, substitutions N83D and A292S are widespread across snake evolutionary history with multiple independent origins and reversals in Colubridae, Elapidae and Lamprophiidae (SI Table S3). The ancestral snake is reconstructed as having an RH1-based pigment with predicted λ_{max} of 493 nm. However, the ancestral colubrine and colubrid *rh1* sequences encode a combination of N83 and S292 (seen in several extant colubroids: Fig. 1), this combination of residues occurs in a species of deep sea fish, *Coryphaenoides guntheri*, with an RH1-based pigment λ_{max} of 479nm (Hunt et al., 2001).

In the *sws1* opsin gene, there are many changes at known spectral tuning sites, notably sites 86, 93, 97, 113 and 118. Mutations at sites 93, 113 and particularly 86 are known to have major effects on SWS1 pigment λ_{max} (Fasick and Robinson 1998; Shi et al. 2001; Cowing et al. 2002; Parry et al. 2004; Yokoyama 2005), but the widespread and multiple substitution T93V has not been reported elsewhere in vertebrates. The T93A substitution found in the vipers *Echis ocellatus* and *Bitis nasicornis* has previously been reported but only in the distantly related snake *Tropidophis feicki* (Simões et al. 2015). The precise effects of these previously unreported substitutions on SWS1 λ_{max} are unknown, but substitutions involving sites 86, 93 and 118 in other vertebrates are known to generate substantial shifts in SWS1 λ_{max} (Parry et al., 2004; Yokoyama et al. 2014; Carvalho et al., 2012). Ancestral reconstruction of *sws1* sequences suggests a UV sensitive (λ_{max} 358-360 nm) SWS1 pigment in the ancestor of several major clades including Alethinophidia, Afrophidia and Colubridae (Fig. 1, SI Table S4).

For the *lws* opsin gene, multiple shifts between predicted λ_{max} of 560nm and 555 nm are widespread across snakes as a consequence of substitution S180A. Additionally, a T285A substitution in combination with S180A further shifts the predicted λ_{max} to 536nm in several snake lineages, notably within the colubrine and dipsadine colubrids (Fig. 1). In *Heterodon nasicus,* an A308S substitution is observed; this substitution is also found in combination with A180 in the mouse and rat LWS sequences (Davies et al., 2012) and in a number of aquatic mammals (Newman and Robinson, 2006). The introduction of a S308A substitution by site directed mutagenesis in mouse LWS produces a 20 nm long-wave shift (Davies et al., 2012), so the presence of S308 in *H. nasicus* would be expected to produce a similar short-wave shift. Ancestors of most major snake lineages are reconstructed as having an LWS pigment λ_{max} of 555 nm, with shifts to shorter wavelength λ_{max} occurring independently on multiple occasions within Colubridae (Fig. 1, SI Table S5).

Phylogenetics

The inferred *rh1* and *sws1* trees (SI Figs. S6–S11) are broadly consistent with recently published snake phylogenies estimated using more neutral markers, irrespective of whether analyses were run using ML or BI or under GTR+G or GTR+G+I. Notable exceptions to relationships found in recent molecular phylogenies of snakes are the nesting of *Lampropeltis* within dipsadine rather than colubrine colurbids (*rh1*), monophyly of the Scolecophia (*rh1*), and non-monophyly of Anomalepididae (*rh1*) and Lamprophiidae (*rh1*, *sws1*). The *lws* tree is less well supported and lacks some monophyletic higher taxa (e.g., Dipsadinae, Natricinae, Colubrinae, Colubroidea) present in the *rh1* and *sws1* trees. *Xylophis* (not sampled in molecular snake phylogenies) is

recovered variably as closely related to some natricines (*lws*) or lying outside most colubroids (*rh1, sws1*).

Adaptive molecular evolution

Values for dN/dS (ω) (SI Table S12) suggest that all three visual opsin genes are under purifying selection (ω_{Rh1}= 0.237; ω_{SWS1}= 0.107; ω_{LWS}= 0.312), indicative of strong functional constraint (Li et al. 1985). Additional tests performed with alternative phylogenetic relationships among dipsadine, colubrine and natricine colubrids yield ω estimates that are not significantly different (data not shown), indicating that these results are robust with respect to this phylogenetic uncertainty.

For the *sws1* opsin gene, branch models (SI Table S12) suggest that non-fossorial (0.112), non-arboreal (0.08), non-aquatic (0.308) and diurnal (0.149) snake lineages have higher ω values then their counterparts (0.062, 0.097, 0.092 and 0.099, respectively). Colubrids have higher ω values (0.119) than non-colubrids (0.088). In the dataset pruned to species for which retinal anatomy is known, ω values are similar between taxa with transmuted (0.117) and non-transmuted cones (0.101) and lower in species with doubles cones (0.097 vs 0.110). The free-ratio model ω values vary between 0.001 and 0.409.

For the *lws* opsin gene ω values are higher in non-fossorial (0.340), arboreal (0.398), non-aquatic (0.308) and diurnal snakes (0.342) than their counterparts (0.016, 0.284, 0.268 and 0.246, respectively). Colubrids have significantly higher ω values (0.422) than non-colubrids (0.193). Higher ω occur in species with transmuted cones (0.543 vs. 0.273) and in species with double cones (0.373 vs 0.245). The free-ratio ω ranges from 0.001–7.1 (SI Table S12).

The *rh1* ω ratios among non-fossorial (0.252), non-arboreal (0.240), aquatic/semiaquatic (0.253) and nocturnal (0.240) snake lineages are higher than for their counterparts (0.161, 0.212, 0.0.229 and 0.141, respectively). Colubrids have higher (0.252) ω ratios than non-colubrids (0.212) whereas ω ratios are lower for the thoroughly fossorial Scolecophidia (0.141) than their sister group Alethinophidia (0.244). The *rh1* opsin gene is inferred to be under less functional constraint in snakes with transmuted, rod-like cones (0.388 vs. 0.212) and in snakes with double cones (0.283 vs 0.190) (SI Table S12).

The free-ratio ω ranges from 0.001–1.73, suggesting positive selection (ω = 1.44) in the Colubridae stem. With branch models, for all opsin genes, separate values for each of the contrasted ecologies and retinal types are a significantly better fit than a single ω value for all snakes when compared by LRT (SI Table S12).

Site models results infer several instances of positive selection at the codon level across the three visual opsin genes present in snakes (SI Table S13). Models 2a and M8 (β&ω) are significant better fit when compared with the simpler models M1a and M7, respectively (SI Table S12).

According to Bayes Empirical Bayes (BEB) implemented in site models M2a and M8 (β&ω) there are two and seven *sws1* amino acid sites that can be inferred to be under positive selection, respectively (SI Table S11). With M8 (β&ω), two of these seven sites (86 and 93) are known to have a substantial impact on SWS1 spectral tuning, and five of the sites are located in trans-membrane (TM) domains (Fig. 2). In *lws*, BEB results infer 12 and 18 amino acid sites under positive selection under models M2a and M8 (β&ω), respectively. Among the 18, two are involved in LWS spectral tuning and two others are located within the retinal pocket (Fig. 2). A total of 15 of the 18 inferred positively selected sites are located in TM domains, particularly TM 3, 4 and 5 (11 sites). In *rh1*, positive selection is inferredd in 11 and 16 amino-acid sites according to M2a and M8 (β&ω) models, respectively. Under model M8 (β&ω), BEB results infer positive selection in spectral sites 83 and 292 and in two sites within the retinal pocket (Fig. 2, SI Table S11). The majority of the *rh1* amino acids inferred to be under positive selection are located in TM domains, especially TM 3, 4, 5 and 7 (Fig. 2). For the results of both M2a and M8 (β&ω) models, chi-squared tests rejected the null that inferred positively selected sites are not located within TMs versus loops more than expected for RH1 and LWS but not for SWS1. Pooling all visual opsins, chi squared-tests also rejected the null hypothesis that inferred positively selected sites are not located within extracellular versus intracellular loops more than expected.

Using PRIME (SI Table S16-S21), positive selection is inferred at amino acid sites at which substitutions with changes in biochemical properties occurred. Among these sites are spectral tuning sites 86 in *sws1* and 180 in *lws*, and amino acid sites situated within the retinal pocket in *lws* and *rh1* (Fig 2).

Ocular media transmission

The sampled snakes have lenses with a broad range of transmission properties at short wavelengths, ranging from those that filter out all of the UV and even some of blue (the lenses thus appearing yellow) to those that transmit most of the UVA (Fig 3A: SI Table S22). All spectacles transmitted the UVA well (Fig 3B), corroborating recent work on 42 snake species by (van Doorn and Sivak 2015). All nocturnal species have very UVA transmissive lenses, while all species with lenses that cut out shorter wavelengths to

varying degrees are diurnal (Fig 3C). However, not all snakes with some diurnal activity have UV-blocking lenses.

Discussion

Walls (1934; 1942) and Underwood (1967) documented extensive diversity in retinal anatomy among snakes. Our results demonstrate that snakes also display remarkable diversity in spectral transmission of the lens and variability in visual opsin gene sequences and visual pigment spectral sensitivity that together point to an evolutionarily complex system.

It has been argued that snakes passed through a nocturnal and/or fossorial stage early in their evolutionary history, with some associated diminution of their visual systems (see Simões et al. 2015) followed by possible re-elaboration in 'higher' snakes (Alethinophidia), including substantial diversification in retinal photoreceptor complements, at least at a morphological level (Walls 1942; Underwood 1967). The results presented here indicate that the complement of visual pigments, in contrast, has remained largely stable through notable evolutionary events such as the acquisition of double cones, the loss of classes of single cone (and perhaps rods), and the transmutations of both rods and cones.

The vast majority of species surveyed express the same three (*rh1, sws1, lws*) visual opsin genes that were likely to have been present in the ancestral snake (Davies et al. 2009; Simões et al. 2015). A striking feature is however the absence of *rh1* in the colubrids *Phyllorhynchus decurtatus, Macroprotodon brevis* and *Malpolon monspessulanus*. Given the good quality of the template cDNA available for these species, this is unlikely to be a PCR artefact. *Malpolon monspessulanus*, a highly diurnal species, is reported to have only cones (Underwood 1967; Underwood 1970) and a previous microspectrophotometric (MSP) study (Govardovskii and Chkheidze 1989) failed to find any visual pigments with a λ_{max} close to the c. 500 nm expected for RH1 pigments (typically occurring in rods). *Phyllorhynchus decurtatus* is nocturnal but its 'rods' have been argued to be transmuted (rod-like) cones (Walls 1934), consistent therefore with the lack of RH1. Among vertebrates, absence of an expressed *rh1* has previously been reported only in another group of squamate reptiles, geckos (e.g. Loew et al. 1996; Yokoyama and Blow 2001). More work examining the physiology of visual pigments and gene expression will be required to test this further for snakes. Among those snakes with three functional visual opsin genes is *Uropeltis* cf. *macrolepis*. Like all uropeltids, this is a mostly fossorial species, though it is more likely to be seen above ground during daylight (D.J.G., pers. obs.) and has a larger eye than the distantly related,

but also burrowing, scolecophidians and *Anilius scytale*, for which Simões et al. (2015) failed to amplify either *sws1* or *lws*. The presence of *sws1* and *lws* in *U.* cf. *macrolepis* adds support to Simões et al. (2015) conclusion that loss of all visual opsins except *rh1* has occurred in snakes in only the most dedicated of burrowers, and that if the ancestral snake was a burrower it was likely not as fossorial as living scolecophidians.

We predict that in snakes where the ocular media filter out most of the UVA (Fig 3A&B, SI Table S22), the SWS1 pigment λ_{max} is long-wave shifted. However, the *sws1* sequences of these species include previously unreported amino acid residues at some key tuning sites so this cannot be confirmed, and direct measurements of visual pigment absorbance (e.g. by MSP) are currently lacking. Nevertheless, evidence from other studies (Carvalho et al., 2012; Cowing et al., 2002; Hunt and Peichl, 2014; Parry et al., 2004; Yokoyama et al., 2005) suggests that the replacement of F86 is sufficient to shift the λ_{max} from UV to violet. So only six of the 60 snakes listed in Table S4 may have lost a UVS SWS1 pigment. Removal of UV has been linked to increased acuity rather than an adaptation underpinning a particular form of colour vision or protection from harmful UV light (Douglas and Jeffery 2014). This hypothesis receives support here because the snakes with the least transparent lenses are highly visual hunters. These include a gliding species (*Chrysopelea ornata*) known to track distant objects (Socha and Sidor 2005) and a taxon (*Ahaetulla*) with horizontal pupils, binocular vision and a fovea (Walls 1942). The latter structure is known from very few snakes (Rasmussen 1990) and is indicative of high visual acuity in a specialised area of the retina.

Based on ancestral state reconstruction for the *sws1* gene (and predictions of λ_{max}), the most recent common ancestor of living snakes was UV sensitive, and UV vision is also predicted to be present in many nocturnal caenophidians, matching the situation in other vertebrate groups (e.g., Veilleux and Cummings 2012) in which nocturnality is associated with UV sensitivity. Although there is evidence of a substantial amount of evolutionary change in snake *sws1* sequences, it is not possible to predict the λ_{max} of the SWS1-based visual pigments in 42 of the 63 species for which sequences are available (many of these species are not primarily nocturnal) because of tuning site amino acid substitutions (or combinations of substitutions) not known in other vertebrates. It is very likely (based on lens transmission) that at least some of these species have substantially long-wave shifted SWS1-based visual pigments. Hart et al. (Hart et al. 2012) found (using MSP) that the probable SWS1-based pigments in two sea snakes is not maximally sensitive in the UV, with λ_{max} of c. 429nm. Although many snakes have previously unknown *sws1* tuning site substitutions, there is evidence that some sequences discovered here produce substantial changes in SWS1 $\lambda_{max.}$ Mutations at site 86 are known to cause major shifts in SWS1 λ_{max}, with F86Y (Fasick and Robinson 1998;

Cowing et al. 2002) and F86S (Shi et al. 2001) short-wave shifting λ_{max} by 66 and 51 nm (Yokoyama 2005) respectively, and the latter mutation is observed in the snakes *Malpolon monspessulanus* and *Pantherophis guttatus.* In *Ahaetulla nasuta*, *Chrysopelea ornata*, *Helicops angulatus* and *Chironius* spp. F86V is observed. The guinea pig has a 86V substitution and an SWS1 λ_{max} of 420nm and, furthermore, the V86F substitution produces one of the most substantial shifts towards the UV with a decrease of 53nm in the SWS1 pigment λ_{max} (Parry et al. 2004). Given the filtering out of UV light by the lens a short-wave shifted λ_{max} would seem very unlikely, otherwise SWS1 would not function as an efficient visual pigment in these snakes.

In *Helicops angulatus*, cloning the *sws1* gene revealed polymorphism at site 86 with either valine or phenylalanine. The exact change in spectral tuning is not known, but, speculatively, this polymorphism indicates that pigments with spectral peaks in the UV and violet may be present simultaneously and potentially may therefore provide the basis for a form of trichromacy. This would be similar to the form of trichromacy in polymorphic female platyrrhine monkeys (Jacobs et al. 2002), if some random allele inactivation is present that ensures only one allele is expressed per photoreceptor. Alternatively, both alleles in *H. angulatus* may be fully active to give a broader spectrum of sensitivity.

There are multiple changes in amino acid sequences at known *rh1* spectral tuning sites, particularly D83N, sometimes in combination with A292S. In isolation the former mutation is known to decrease λ_{max} by c. 6nm (Nathans 1990) and the latter by c. 10nm (Janz and Farrens 2001). Some deep sea fish species have both N93 and S292 with λ_{max} varying between 468 and 489 nm (Hunt et al. 2001) and MSP data for the natricine snake *Thamnophis sirtalis* (Sillman et al. 1997) indicates that the likely RH1-based visual pigment has a λ_{max} at 481nm (Hunt et al. 2001). This suggests that, combined, the two mutations potentially short-wave shift the rod visual pigment λ_{max} by c. 18nm, though other sites and mechanisms might also be involved. The other 21 snake species with *rh1* N83 and S292 (SI Table S3) would be expected to have similar λ_{max} values.

In contrast to *rh1* and *sws1,* the *lws* spectral sites in snakes are identical to those known in other vertebrates, with the exception of the A308S substitution unique to the colubrine *Heterodon nasicus*. Variation in the amino acid residues at LWS spectral sites in snakes suggests multiple LWS λ_{max} shifts between and within long (555-560nm) and medium wavelengths (536-543nm) within Caenophidia. Substitutions are particularly common in Dipsadinae and Colubrinae, with most shifts to predicted shorter wavelength λ_{max} values occurring in nocturnal taxa, thereby providing a possible adaptation to maximize photon capture and potentially colour vision in low light conditions. In a study of forest mammals, (Veilleux and Cummings 2012) found that SWS

582 spectral tuning appeared to be strongly associated with foraging target and LWS tuning
583 to dominant light field characteristics. Although the shorter wavelength shifted LWS λ_{max}
584 values of nocturnal snakes match this, we are unable to address whether snake SWS1 is
585 more tuned to foraging targets because SWS1 λ_{max} is not known for most snakes (see
586 above), dietary classification is non-trivial, and many snakes are probably primarily using
587 olfaction rather than visual clues to detect prey

588 The results of our analyses of positive selection in snake visual opsins are notable
589 on two counts. Firstly, unlike some other studies of vertebrate visual opsins (e.g.
590 Yokoyama et al. 2008) we infer multiple sites as under positive selection in all three
591 visual opsins and some of these occur in sites of known functional importance, including
592 known spectral tuning sites. This is consistent with the interpretation that the tuning of snake
593 LWS pigments is influenced by positive selection at sites known to be important in effecting
594 tuning variation in many other vertebrate groups (Hunt and Collin 2014). Secondly, shifts in
595 the molecular evolution (functional constraint) of the visual pigment genes are
596 correlated with many variables, including ecological niche characteristics and retinal
597 anatomy. That the inferred functional constraint is lower in all visual opsin genes in
598 snakes with transmuted, rod-like cones is an important observation indicating that
599 visual pigment adaptation occurs in association with morphological transmutation of
600 photoreceptors — an incompletely understood process with poorly known functional
601 outcomes (Simões et al, 2016). Although we found evidence for less functional
602 constraint in the evolution of *rh1* and *lws* (but not *sws1*) in lineages with double cones,
603 this is difficult to interpret because the function of double cones remains largely
604 unknown (e.g. Pignatelli et al. 2010).

605 Of the three visual opsins found in snakes, *sws1* has fewer amino acid sites
606 inferred to be under positive selection, consistent with higher purifying selection
607 estimates on branch models (SI Table S12) and possibly indicating possibly greater
608 purifying selection than in *lws* and *rh1*. This is consistent with the relatively few tuning
609 sites identified in SWS1 opsins. Indeed, two of the seven *sws1* sites inferred to be under
610 positive selection are the spectral tuning sites 86 and 93 known to impart substantial
611 λ_{max} shifts (Fasick and Robinson 1998; Shi et al. 2001; Yokoyama 2005), suggestive of at
612 least some localized positive selection on sites of functional importance. Similarly, *lws*,
613 sites 180 and 285 and *rh1* sites 83 and 292 are inferred to be under positive selection
614 and also mediate important changes in λ_{max} of their respective pigments (see above).
615 Thus, some of the evolution of snake visual opsins inferred here is interpreted as likely
616 adaptive change related to spectral tuning of pigments. Colour vision has yet to be
617 demonstrated behaviourally in snakes, but our results suggest it is almost certainly an
618 important part of their sensory biology, especially for many caenophidians. The visual

pigment complement of most snakes, comprising RH1, SWS1 and LWS based pigments, is strongly suggestive of photopic cone dichromacy and scotopic monochromacy as found in most mammals. However, there remains the possibility of trichromacy, either by the involvement of transmuted cone-like rods in the case of diurnal species (Schott et al. 2016), or by the use of transmuted rod-like cones in nocturnal species (as occurs in geckos: Roth & Kelber 2004). As with the observed polymorphism of *lws* found in *Helicops angulatus*, further studies are required to elucidate these possibilities and the consequences of different visual pigment complements in snake colour vision.

Most of the amino acid sites inferred to be under positive selection in the three visual opsin genes found in snakes are in transmembrane domains (Fig. 3), and most observed changes at these sites are non-conservative in terms of amino acid properties (Fig. 2, SI Table S13). Transmembrane domains impact the tertiary structure, thermal stability (Kobilka 2007) and aspects of the retinal binding pocket (Yokoyama et al. 2006) of the opsin, such that positive selection at these sites is likely to have major influence on opsin function. Change in spectral tuning is only one of the possible functional outcomes of visual opsin amino acid substitutions - there is more to visual pigments than spectral absorption - and these other aspects of visual sensory transduction will need to be part of the future investigations of this system.

Conclusion

Based on surveys of retinal anatomy, the eyes of snakes have been cited as one of the most interesting cases of visual adaptation among vertebrates (Walls 1942; Underwood 1967), but they remained overlooked during the revolution in molecular analyses of visual pigment genes. Our results show that in addition to the substantial anatomical diversity, snakes also have notable diversity in their lens transmission and visual opsin genes, including diversity not known in other vertebrates, and these aspects of snake vision are shown to have undergone considerable evolution. Snake visual opsin genes contain signals of positive selection in sites of functional importance that are (perhaps causally) associated with shifts in ecology and retinal anatomy. We conclude that the diversity, function and evolution of snake vision are worthy of additional research, and that understanding of vertebrate vision is incomplete without a consideration of snakes.

Acknowledgements

This work was funded by a grant from the Leverhulme Trust (RPG-342 to DJG, NSH, DMH & JCP). Permits for research and export were granted by Direction de l'Environment de l'Aménagement

et du Logement and the Direction des Services Vétérinaires de la Guyane, Cayenne, French Guiana, and by the Ministry of Forestry & Wildlife of Cameroon. For assistance in the field, we thank Gabriela Bittencourt-Silva, Antoine Fouquet, Philippe Gaucher, Jeannot and Odette (Camp Patawa) and Mark Wilkinson. Additional practical assistance with obtaining and processing samples, and with literature and analysis was provided by Christian Cox, Vivek Philip Cyriac, David Donaire, Robert Fisher, Varad Giri, Rachunliu G. Kamei, Panagiotis Kornilios, Marcel Kouete, Dileep Kumar, Michelle Lawing, Mruganka Rahul Lele, Gopal Murali, Jesse Meik, Simon Maddock, Bartosz Nadol, David Richards, Gill Sparrow, Jeff Streicher, Colin Strine, Ed Wade, Chris Williamson, Mark Wilkinson, and the NHM Sequencing Facility, and we thank them all. Chris Hull provided help with the smoothing of the ocular media transmission data.

References

Atchley WR, Zhao J, Fernandes AD, Drüke T. 2005. Solving the protein sequence metric problem. Proc Natl Acad Sci. 102:6395–6400.

Bowmaker J, Hunt D. 2006. Evolution of vertebrate visual pigments. Curr Biol. 16:R484–R849.

Carleton KL, Hofmann CM, Klisz C, Patel Z, Chircus LM, Simenauer LH, Soodoo N, Albertson RC, Ser JR. 2010. Genetic basis of differential opsin gene expression in cichlid fishes. J Evol Biol. 23:840–853.

Conant GC, Wagner GP, Stadler PF. 2007. Modeling amino acid substitution patterns in orthologous and paralogous genes. Mol Phyl and Evol. 42:298–307.

Cowing JA, Poopalasundaram S, Wilkie SE, Robinson PR, Bowmaker JK, Hunt DM. 2002. The molecular mechanism for the spectral shifts between vertebrate ultraviolet- and violet-sensitive cone visual pigments. Biochem J. 367:129.

Darriba D, Taboada GL, Doallo R, Posada D. 2012. jModelTest 2: more models, new heuristics and parallel computing. Nat Methods 9:772.

Davies WIL, Collin SP, Hunt DM. 2012. Molecular ecology and adaptation of visual photopigments in craniates. Mol Ecol. 21:3121–3158.

Davies WL, Cowing JA, Bowmaker JK, Carvalho LS, Gower DJ, Hunt DM. 2009. Shedding Light on Serpent Sight: The Visual Pigments of Henophidian Snakes. J Neurosci. 29:7519–7525.

Delport W, Poon AFY, Frost SDW, Kosakovsky Pond SL. 2010. Datamonkey 2010: a suite of phylogenetic analysis tools for evolutionary biology. Bioinformatics. 26:2455–2457.

690 Delport W, Scheffler K, Botha G, Gravenor MB, Muse SV, Kosakovsky Pond SL. 2010.
691 CodonTest: Modeling Amino Acid Substitution Preferences in Coding Sequences. PLoS
692 Comput Biol 6:e1000885.

693 Douglas RH, Jeffery G. 2014. The spectral transmission of ocular media suggests
694 ultraviolet sensitivity is widespread among mammals. *Proc R Soc. B* 281:20132995–
695 20132995.

696 Douglas RH, Marshall NJ. 1999. A review of vertebrate and invertebrate ocular filters. In:
697 Adaptive Mechanisms in the Ecology of Vision. Dordrecht: Springer Netherlands. pp. 95–
698 162.

699 Douglas RH, McGuigan CM. 1989. The spectral transmission of freshwater teleost ocular
700 media – an interspecific comparison and a guide to potential ultraviolet sensitivity.
701 Vision Res. 29:871–879.

702 Dulai K, Dornum M, Mollon J, Hunt D. 1999. The Evolution of Trichromatic Color Vision
703 by Opsin Gene Duplication in New World and Old World Primates. Genome Res. 9:629–
704 638.

705 Edgar, RC. 2004. MUSCLE: multiple sequence alignment with high accuracy and high
706 throughput. *Nucleic Acids Res*. 32: 1792–1797.

707 Enright JM, Toomey MB, Sato S-Y, Temple SE, Allen JR, Fujiwara R, Kramlinger VM, Nagy
708 LD, Johnson KM, Xiao Y, et al. 2015. Cyp27c1 Red-Shifts the Spectral Sensitivity of
709 Photoreceptors by Converting Vitamin A1 into A2. Curr Biol. 25: 1-10.

710 Fasick JI, Robinson PR. 1998. Mechanism of spectral tuning in the dolphin visual
711 pigments. Biochemistry 37:433–438.

712 Gans C. 1982. The Sri Lankan genus Aspidura (Serpentes, reptilia, Colubridae) (Annals of
713 Carnegie Museum). Carnegie Museum of Natural History

714 Govardovskii VI, Chkheidze NI. 1989. Retinal photoreceptors and visual pigments in
715 certain snakes. Biol Abstr. 90:1036.

716 Gower DJ, Winkler JD. 2007. Taxonomy of the Indian snake Xylophis Beddome
717 (Serpentes: Caenophidia), with description of a new species. Hamadryad 31:315–329.

718 Hart NS, Coimbra JP, Collin SP, Westhoff G. 2012. Photoreceptor types, visual pigments,
719 and topographic specializations in the retinas of hydrophiid sea snakes. J Comp Neurol
720 520:1246–1261.

721 Hauser FE, van Hazel I, Chang BSW. 2014. Spectral tuning in vertebrate short
722 wavelength-sensitive 1 (SWS1) visual pigments: Can wavelength sensitivity be inferred
723 from sequence data? J Exp Zool B Mol Dev Evol. 322:529–539.

Hofmann CM, Carleton KL. 2009. Gene Duplication and Differential Gene Expression Play an Important Role in the Diversification of Visual Pigments in Fish. Integr Comp Biol. 49:630.

Huelsenbeck JP, Ronquist F. 2001. MRBAYES: Bayesian inference of phylogenetic trees. Bioinformatics 17:754–755.

Hunt DM, Collin SP. 2014. Evolution of Visual and Non-visual Pigments. In: Hunt DM, Hankins MW, Collin SP, Marshall NJ, editors. Evolution of Visual and Non-visual Pigments. Boston, MA: Springer. p. 276.

Hunt DM, Dulai KS, Partridge JC, Cottrill P, Bowmaker JK. 2001. The molecular basis for spectral tuning of rod visual pigments in deep-sea fish. J Exp Biol. 204:3333–3344.

Jacobs G, II J, Tan Y, Li W-H. 2002. Opsin gene and photopigment polymorphism in a prosimian primate. Vision Res. 42:11–18.

Janz JM, Farrens DL. 2001. Engineering a Functional Blue-Wavelength-Shifted Rhodopsin Mutant†. Biochemistry 40:7219–7227.

Katoh K, Misawa K, Kuma K, Miyata T. 2002. MAFFT: a novel method for rapid multiple sequence alignment based on fast Fourier transform. Nucleic Acids Res. 30:3059–3066.

Kearse M, Moir R, Wilson A, Stones-Havas S, Cheung M, Sturrock S, Buxton S, Cooper A, Markowitz S, Duran C, et al. 2012. Geneious Basic: an integrated and extendable desktop software platform for the organization and analysis of sequence data. Bioinformatics 28:1647–1649.

Kobilka BK. 2007. G protein coupled receptor structure and activation. Biochimica et Biophysica Acta (BBA) - Biomembranes 1768:794–807.

Kondrasiv SL, Gamburzena AG, Gnjibkina VP, Orlov OJ, My PT. 1986. Coloration of corneas in fish. A list of species. Vision Res. 26:287–290.

Land MF. 1981. Optics and vision in invertebrates. In: Autrum HJ, editor. Handbook of Sensory Physiology. Vol. VII/6B. Berlin. pp. 471–592.

Li WH, Wu CI, Luo CC. 1985. A new method for estimating synonymous and nonsynonymous rates of nucleotide substitution considering the relative likelihood of nucleotide and codon changes. Mol Biol Evol. 2:150–174.

Loew ER, Govardovskii VI, Rohlich P, Szél A. 1996. Microspectrophotometric and immunocytochemical identification of ultraviolet photoreceptors in geckos. Vis Neurosci. 13:247–256.

Löytynoja A & Goldman N. 2005. An algorithm for progressive multiple alignment of

757 sequences with insertions. *Proc Nat Acad Sci*, *102*(30): 10557–10562.

758 Martin M, Le Galliard J-F, Meylan S, Loew ER. 2015. The importance of ultraviolet and
759 near-infrared sensitivity for visual discrimination in two species of lacertid lizards. J Exp
760 Biol. 218:458–465.

761 McDowell SB. 1987. Systematics. In: Seigel RA, Collins JT, Novak SS, editors. Snakes:
762 Ecology and Evolutionary Biology. New York. pp. 3–50.

763 Nathans J. 1990. Determinants of Visual Pigment Absorbance: Role of Charged Amino
764 Acids in the Putative Transmembrane Segments. Biochemistry 29:937.

765 Nickle B, Robinson PR. 2007. The opsins of the vertebrate retina: insights from
766 structural, biochemical, and evolutionary studies. Cell Mol Life Sci 64:2917–2932.

767 Nilsson DE. 1996. Eye ancestry: old genes for new eyes. Curr Biol. 6:39–42.

768 Parry J, Poopalasundaram S, Bowmaker J, Hunt D. 2004. A Novel Amino Acid
769 Substitution Is Responsible for Spectral Tuning in a Rodent Violet-Sensitive Visual
770 Pigment. Biochemistry 43:8014–8020.

771 Pattengale ND, Alipour M, Bininda-Emonds ORP, Moret BME, Stamatakis A. 2009. How
772 Many Bootstrap Replicates Are Necessary? In: Springer-Verlag. pp. 184–200.

773 Pignatelli V, Champ C, Marshall J, Vorobyev M. 2010. Double cones are used for colour
774 discrimination in the reef fish, Rhinecanthus aculeatus. Biol Lett. 6:537–539.

775 Pyron R, Burbrink FT, Wiens JJ. 2013. A phylogeny and revised classification of
776 Squamata, including 4161 species of lizards and snakes. BMC Evol Biol. 13:93.

777 Rasmussen JB. 1990. The retina of Psammodynastes pulverulentus (Boie, 1827) and
778 Telescopus fallax (Fleischmann, 1831) with a discussion of their phylogenetic
779 significance (Colubroidea, Serpentes). J Zool Syst Evolut. 28:269–276.

780 Reeder TW, Townsend TM, Mulcahy DG, Noonan BP, Wood PL, Sites JW, Wiens JJ. 2015.
781 Integrated Analyses Resolve Conflicts over Squamate Reptile Phylogeny and Reveal
782 Unexpected Placements for Fossil Taxa. PLoS ONE 10:e0118199.

783 Schott RK, Müller J, Yang CGY, Bhattacharyya N , Chan N, Xu M, et al. 2015. Evolutionary
784 transformation of rod photoreceptors in the all-cone retina of a diurnal garter snake.
785 *Proc Nat Acad Sci USA*, 201513284.

786 Shi Y, Radlwimmer FB, Yokoyama S. 2001. Molecular genetics and the evolution of
787 ultraviolet vision in vertebrates. Proc Natl Acad Sci. 98:11731–11736.

788 Siebeck UE, Marshall NJ. 2000. Transmission of ocular media in labrid fishes. Phil. Trans.

789 Royal Soc B: Biol Sc. 355:1257–1261.

790 Sillman AJ, Govardovskii VI, Rohlich P, Southard JA, Loew ER. 1997. The photoreceptors
791 and visual pigments of the garter snake (Thamnophis sirtalis): a
792 microspectrophotometric, scanning electron microscopic and immunocytochemical
793 study. J Comp Physiol A 181:89.

794 Simões BF, Sampaio FL, Jared C, Antoniazzi MM, Loew ER, Bowmaker JK, Rodriguez A,
795 Hart NS, Hunt DM, Partridge JC, et al. 2015. Visual system evolution and the nature of
796 the ancestral snake. J Evol Biol. 28:1309–1320.

797 Simões, B. F., Sampaio, F. L., Loew, E. R., Sanders, K. L., Fisher, R. N., Hart, N. S., et al.
798 (2016). Multiple rod-cone and cone-rod photoreceptor transmutations in snakes:
799 evidence from visual opsin gene expression. Proc R Soc. B 283: 1823.

800 Stamatakis A. 2014. RAxML version 8: a tool for phylogenetic analysis and post-analysis
801 of large phylogenies. Bioinformatics 30:1312–1313.

802 Team RC. 2014. R: A language and environment for statistical computing. Vienna,
803 Austria: R Foundation for Statistical Computing

804 Thorpe A. 1991. Spectral trtansmission and short–wave absorbing pigments in the
805 lenses of fish and other animals. City University, London.

806 Underwood G. 1967. A Contribution to the Classification of Snakes. British Museum
807 Natural History Publications

808 Underwood G. 1970. The Eye. In: Gans C, Parsons TS, editors. Biology of the Reptilia:
809 Morphology B. Vol. 2. New York: Academic Press. pp. 1–97.

810 van Doorn K, Sivak JG. 2015. Spectral transmittance of the spectacle scale of snakes and
811 geckos. Contrib Zool. 8:1–12.

812 Veilleux CC, Cummings ME. 2012. Nocturnal light environments and species ecology:
813 implications for nocturnal color vision in forests. J Exp Biol. 215:4085–4096.

814 Wald G. 1968. The molecular basis of visual excitation. Nature. 219:800–807.

815 Walls GL. 1931. The Occurrence of Colored Lenses in the Eyes of Snakes and Squirrels,
816 and Their Probable Significance. Copeia 1931:125–127.

817 Walls GL. 1934. The reptilian retina. I. A new concept of visual cell evolution. Am J
818 Ophthalmol. 17:892–915.

819 Walls GL. 1942. The Vertebrate Eye and Its Adaptive Radiation. New York: Fafner
820 Publishing Company

Wickham H. 2010. ggplot2. New York, NY: Springer

Wiens JJ, Hutter CR, Mulcahy DG, Noonan BP, Townsend TM, Sites JW, Reeder TW. 2012. Resolving the phylogeny of lizards and snakes (Squamata) with extensive sampling of genes and species. Biol Lett. 8:1043–1046.

Yang Z. 1998. Likelihood ratio tests for detecting positive selection and application to primate lysozyme evolution. Mol Biol Evol. 15:568–573.

Yang, Z. 2006. Computational molecular evolution. Oxford University Press, USA.

Yang Z. 2007. PAML 4: Phylogenetic Analysis by Maximum Likelihood. Mol Biol Evol. 24:1586–1591.

Yang ZH, Nielsen R, Goldman N, Pedersen A. 2000. Codon-substitution models for heterogeneous selection pressure at amino acid sites. Genetics 155:431–449.

Yang ZH, Wong W, Nielsen R. 2005. Bayes Empirical Bayes Inference of Amino Acid Sites Under Positive Selection. Mol Biol Evol. 22:1107.

Yokoyama S, Blow NS. 2001. Molecular evolution of the cone visual pigments in the pure rod-retina of the nocturnal gecko, Gekko gekko. Gene 276:117–125.

Yokoyama S, Starmer WT, Takahashi Y, Tada T. 2006. Tertiary structure and spectral tuning of UV and violet pigments in vertebrates. Gene 365:95–103.

Yokoyama S, Tada T, Zhang H, Britt L. 2008. Elucidation of phenotypic adaptations: Molecular analyses of dim-light vision proteins in vertebrates. Proc Natl Acad Sci. 105:13480–13485.

Yokoyama S, Xing J, Liu Y, Faggionato D, Altun A, Starmer WT. 2014. Epistatic Adaptive Evolution of Human Color Vision. PLoS Genet. 10:e1004884.

Yokoyama S. 2005. Elephants and Human Color-Blind Deuteranopes Have Identical Sets of Visual Pigments. Genetics 170:335–344.

Yokoyama S. 2008. Evolution of Dim-Light and Color Vision Pigments. Annu Rev Genomics Hum Genet. 9:259–282.

Zhang J. 2005. Evaluation of an Improved Branch-Site Likelihood Method for Detecting Positive Selection at the Molecular Level. Mol Biol Evol. 22:2472–2479.

	SWS1	Rh1	LWS
	357-360	493-499	536-560
Typhlophis squamosus	×[1]	493	×[1]
Liotyphlops beui	×[1]	493	×[1]
Epictia collaris	×[1]	493	×[1]
Amerotyphlops brongersmianus	×[1]	493	×[1]
Anilius scytale	×[2]	493	×[2]
Tropidophis feicki	■	493	555
Gongylophis conicus	360	493	555
Melanophidium khairei	360	493	×
Uropeltis cf. *macrolepis*	■	493	560
Xenopeltis unicolor	360	493	560
Python bivittatus	360	493	560
Python regius	360	493	560
Acrochordus javanicus	■	493	560
Pareas monticola	×	493	×
Bitis nasicornis	■	493	555
Echis ocellatus	■	493	555
Causus rhombeatus	■	493	555
Enhydris innominata	■	493	560
Ophiophagus hannah	■	●	560
Naja kaouthia	■	493	560
Malpolon monspessulanus	■|●	×[4]	560
Polemon collaris	■	●	560
Lamprophis olivaceus	■	499	555
Lycophidion laterale	■	493	555
Mehelya sp.	■	493	536
Amphiesma stolata	■	●	560
Xenochrophis piscator	■	●	560
Natriciteres sylvatica	360	499	560
Xylophis captaini	360	●	555
Natrix maura	357	●	555
Thamnophis sirtalis	●	●	555
Heterodon nasicus	357	●	■
Erythrolamprus reginae	357	493	560
Helicops angulatus	■|●	493	555
Thamnodynastes pallidus	■	●	555
Xenopholis scalaris	357	493	536
Pseudoboa coronata	■	499	555
Oxyrhopus melanogenys	■	499	555
Hypsiglena jani	357	493	543
Imantodes lentiferus	■|●	493	536
Leptodeira annulata	357	493	535
Atractus badius	357	●	536
Atractus flammigerus	357	499	536
Sibon nebulatus	357	499	536
Dipsas indica	357	499	536
Dipsas catesbyi	357	499	536
Ahaetulla nasuta	■|●	●	560
Chrysopelea ornata	■|●	●	560
Telescopus fallax	■	493	536
Boiga forsteni	×	493	543
Dasypeltis scabra	■	493	536
Boiga ceylonensis	×	×	543
Macroprotodon brevis	357	×	555
Spalerosophis diadema	■|●	●	555
Hemorrhois hippocrepis	■	●	560
Opheodrys aestivus	■|●	499	560
Chironius fuscus	■|●	●	560
Chironius carinatus	■|●	●	560
Pseustes poecilonotus	■|●	●	560
Phyllorynchus decurtatus	■	×	555
Lycodon aulicus	■|●	493	536
Orthriophis taeniurus	■|●	493	555
Elaphe climacophora	■|●	●	555
Pantherophis guttatus	■|●	493	536
Pituophis catenifer	■	●	536
Bogertophis subocularis	■	●	536
Arizona elegans	■|●	●	536
Lampropeltis californiae	■|●	499	555
Lampropeltis floridiana	■|●	499	555

λ_{max} (nm)

① ② ③ ④ ⑤ ⑥ ⑦ ⑧ ⑨ ⑩

357 493 555

357 493 560

357 493 555

357 493 560

357 ● 560

357 ● 555

357 ● 560

Yes No

Primarily Fossorial

(Semi)Aquatic

Primarily Arboreal

Primarily Diurnal

Transmuted Cones

Double Cones

× Not amplified

■ Spectral site with unknown λ_{max}

● Spectral sites interaction with unknown λ_{max}

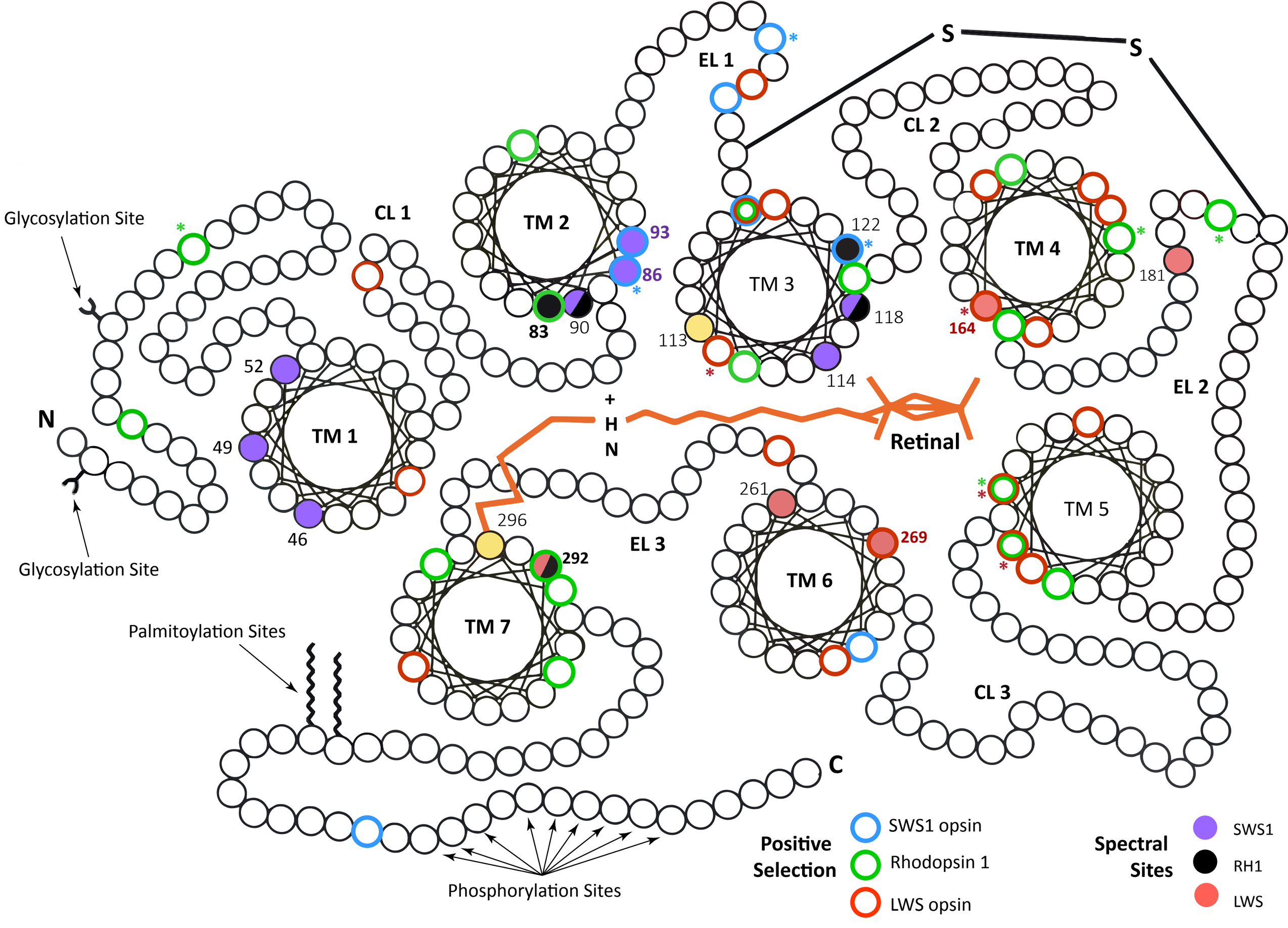
Glycosylation Site
CL 1
TM 2
EL 1
S
S
CL 2
TM 4
TM 3
122
118
113
114
93
86
83
90
181
164
EL 2
N
52
TM 1
49
46
Glycosylation Site
+
H
N
Retinal
296
292
EL 3
261
269
TM 6
TM 5
TM 7
CL 3
Palmitoylation Sites
C
Phosphorylation Sites
Positive Selection
SWS1 opsin
Rhodopsin 1
LWS opsin
Spectral Sites
SWS1
RH1
LWS

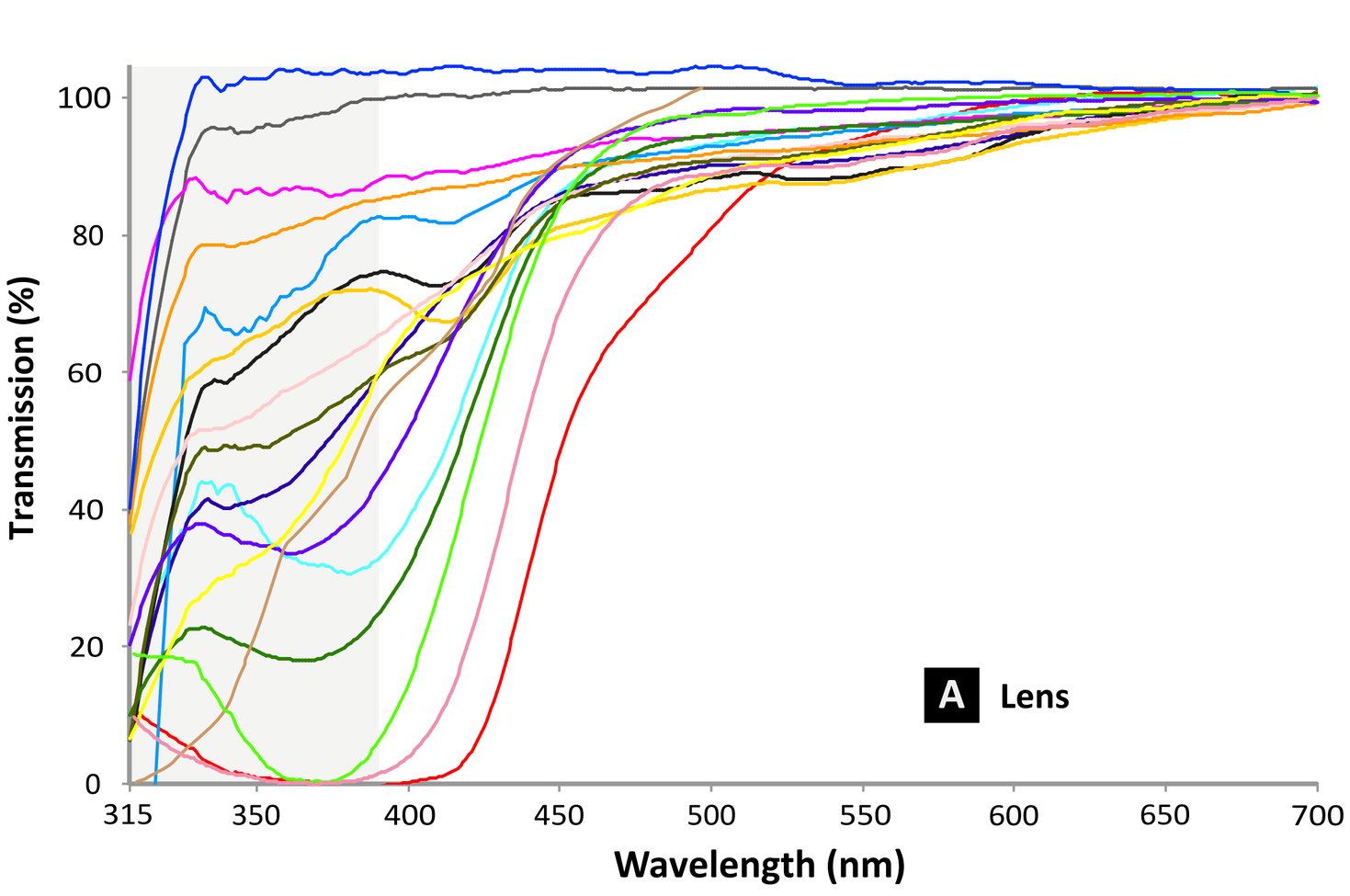
Transmission (%)
100
80
60
40
20
0
315
350
400
450
500
550
600
650
700
Wavelength (nm)
A Lens

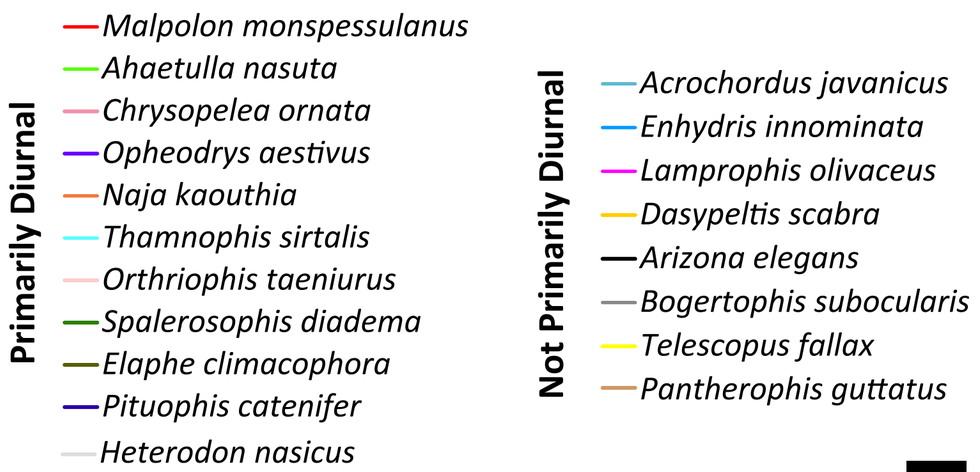
Primarily Diurnal
Malpolon monspessulanus
Ahaetulla nasuta
Chrysopelea ornata
Opheodrys aestivus
Naja kaouthia
Thamnophis sirtalis
Orthriophis taeniurus
Spalerosophis diadema
Elaphe climacophora
Pituophis catenifer
Heterodon nasicus
Not Primarily Diurnal
Acrochordus javanicus
Enhydris innominata
Lamprophis olivaceus
Dasypeltis scabra
Arizona elegans
Bogertophis subocularis
Telescopus fallax
Pantherophis guttatus

Transmission (%)
100
80
60
40
20
0
315
350
400
450
500
550
600
650
700
Wavelength (nm)
UV
Visible
B Spectacle

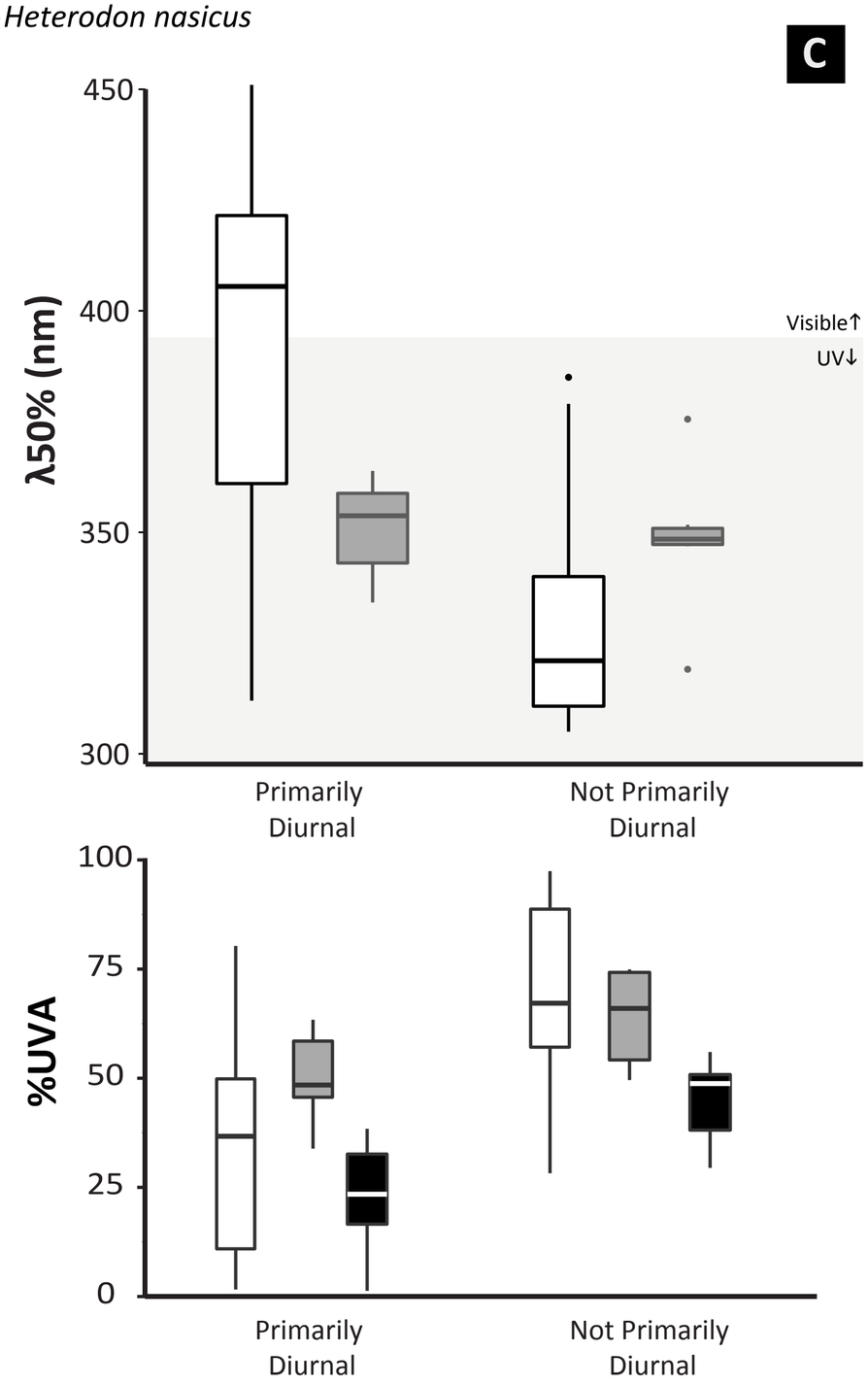
C
λ50% (nm)
450
400
350
300
Visible↑
UV↓
Primarily Diurnal
Not Primarily Diurnal
%UVA
100
75
50
25
0
Primarily Diurnal
Not Primarily Diurnal

FIGURE CAPTIONS

Figure 1. Snake species tree and phenotypic classifications (see Material and Methods for more information) used in analyses of opsin gene evolution. Numbers within circles represent snake higher taxa: ①Scolecophidia (not recovered in some molecular phylogenies); ②Alethinophidia; ③Henophidia (not recovered in molecular phylogenies); ④ Afrophidia; ⑤ Caenophidia; ⑥Viperidae; ⑦Colubridae, ⑧Natricinae ⑨Dipsadinae; ⑩Colubrinae. Phenotype classifications shown for ecology (squares) and visual cell patterns (circles), with empty circles representing species for which state is unknown and strikethrough circles species with retinas with no cones. Visual pigment peak absorbance (λ_{max}) values for each visual pigment are those predicted from cDNA sequences except where indicated. Ancestral pigment λ_{max} values are shown at selected internal branches in order SWS1-RH1-LWS. 1) SWS1 and LWS pigments have not been detected by MSP for any scolecophidian, and no cones have been found in anatomical studies (see Simões et al. 2015); 2) Anatomical studies have not been carried out for *Anilius scytale* but MSP in this species detected only a single visual pigment (RH1: Simões et al. 2015); 3) No visual pigment with an RH1-like λ_{max} was detected by MSP for *Malpolon* (Govardovski & Chkheidze 1989).

Figure 2. Two-dimensional diagram illustrating the arrangements of the seven transmembrane (TM) domains in visual opsins around the retinal chromophore (based on (Bowmaker and Hunt 2006)). Numbering of amino acid sites is based on bovine rhodopsin. Sites known to dictate spectral tuning are shown for each of the three visual pigments found in snakes, as well sites inferred to be under positive selection estimated by Bayes Empirical Bayes (model M8 β&ω). Sites inferred to be under positive selection associated with biochemical changes (detected by PRIME, SI Table S16-21) are marked with an asterisk (*). EL and CL are extra- and intracellular loops, respectively.

Figure 3. Spectral transmission curves for sampled snakes for (A) lenses and (B) spectacles, and (C) box-plots showing wavelength at which ocular media transmit 50% of the incident illumination (λ50%, top), and the proportion of UVA (315–400 nm) transmission (%UVA, bottom). The box plots summarise data for the lens (white), spectacle (grey) and lens + spectacle (black). Boxes extend from first (Q1) to third quartile (Q3); median is indicated as a horizontal line; whiskers extend to the observation that is closest to, but not more than, a distance of 1.5 (Q3 – Q1) from the

888 end of the box; outliers more distant than this are shown individually. All data newly
889 generated for this study except for *Pantherophis guttatus* (data from Thorpe 1991).